

Strong coupling theory for the Hubbard model

A. Dorneich, M. G. Zacher, C. Gröber and R. Eder

Institut für Theoretische Physik, Universität Würzburg, Am Hubland, 97074 Würzburg, Germany
(November 16, 2016)

We reanalyze the Hubbard-I approximation by showing that it is equivalent to an effective Hamiltonian describing Fermionic charge fluctuations, which can be solved by Bogoliubov transformation. As the most important correction in the limit of large U and weak spin correlations we augment this Hamiltonian by further effective particles, which describe composite objects of a Fermionic charge fluctuation and a spin-, density- or η excitation. The scheme is valid for positive and negative U . We present results for the single particle Green's function for the two-dimensional Hubbard model with and without t' and t'' terms, and compare to Quantum Monte-Carlo (QMC) results for the paramagnetic phase. The overall agreement is significantly improved over the conventional Hubbard-I or two-pole approximation.

71.27.+a,71.10.Fd,71.10.-w

I. INTRODUCTION

The Hubbard model is the simplest system which presumably incorporates the key features of the strong correlation limit. Understanding this model will be crucial for making any progress with cuprate superconductors, colossal magneto resistance systems or Heavy Fermions. The special problem in this model is that near half-filling it represents a dense system of strongly interacting Fermions, a situation in which a perturbation expansion in U may not be expected to give any meaningful results. In dealing with this model, one can then pursue two opposing strategies: one might expect that despite the strong interaction a perturbation expansion in U remains a meaningful approximation, and apply conventional many-body theory. The latter means that one is treating the kinetic energy exactly, and results in the validity of the Luttinger theorem. On the other hand, by adiabatic continuity this approach will never produce an insulator at half-filling so that we can be sure of its breakdown in the limit of large U/t .

The opposite point of view was taken by Hubbard [1,2]: in his approximations, the interaction part of H is treated exactly and approximations are made to the kinetic energy. This results in the breakdown of the Luttinger theorem, because the physical electron is effectively split into two particles, one of them corresponding to an electron moving between empty sites, the other to an electron moving between sites occupied by an electron of opposite spin. The energies of formation of these effective particles differ by U , whence for large U the single free-electron band splits up into two bands formed predominantly by the two types of effective particles. Hubbard's approximations, and related schemes like the so-called 2-pole approximations [3–6], have been dismissed by some authors as unphysical, because they do in fact violate the Luttinger theorem away from half-filling. However, in a recent QMC study for the paramagnetic phase of the

Hubbard model [7] we have shown that such criticism is entirely unwarranted: the Fermi surface, if measured in an 'operational way' from the Fermi energy crossings of the quasiparticle band, indeed does violate the Luttinger theorem. The doping dependence of the Fermi surface volume is qualitatively consistent with Hubbard's results and the main discrepancy being the fact that one can rather clearly distinguish 4 'bands' in the spectral functions rather than the 2 bands predicted by the Hubbard-I approximation. More generally, exact diagonalization studies [8] tend to produce for example a photoemission spectrum consisting of a relatively narrow 'quasiparticle band' (which forms the first ionization states) and an 'incoherent continuum'. A simple two-band form of the spectrum, as produced by the Hubbard-I approximation, therefore cannot give a quantitative description of the spectrum. Motivated by these numerical results we have re-examined the Hubbard I approximation and attempted to find the most important corrections to this scheme for the limit of large U and weak spin correlations. We will see that the 4-band structure observed in the QMC simulations can be reproduced quite well by adding two new effective particles which correspond to a composite object of a 'Hubbard quasiparticle' and a spin-, charge-, or η -excitation. These composite objects actually are the quite obvious leading correction over the Hubbard-I approximation, and we will see that including them into the equations of motion leads to an almost quantitative agreement with the numerical results for a variety of different systems.

II. A REFORMULATION OF THE HUBBARD I APPROXIMATION

We consider the Hubbard Hamiltonian in particle-hole symmetric form, $H = H_t + H_U$ with:

$$H_t = -t \sum_{\langle i,j \rangle} (c_{i,\sigma}^\dagger c_{j,\sigma} + H.c.),$$

$$H_U = U \sum_i (n_{i,\uparrow} - \frac{1}{2})(n_{i,\downarrow} - \frac{1}{2}). \quad (1)$$

Here $\langle i,j \rangle$ denotes summation over all pairs of nearest neighbors and $n_{i,\sigma} = c_{i,\sigma}^\dagger c_{i,\sigma}$.

For bipartite lattices one can make use of two symmetry transformations. The first one is the particle-hole transformation: $c_{i,\sigma} \leftrightarrow e^{i\mathbf{Q}\cdot\mathbf{R}_i} c_{i,\sigma}^\dagger$, where $\mathbf{Q} = (\pi, \pi, \dots, \pi)$. If the kinetic energy contains only nearest neighbor hopping, this transformation leaves the Hamiltonian invariant and exchanges the electron addition spectrum for momentum \mathbf{k} and removal spectrum for momentum $\mathbf{k} + \mathbf{Q}$ at half-filling. Similarly the transformation $c_{i,\downarrow} \leftrightarrow e^{i\mathbf{Q}\cdot\mathbf{R}_i} c_{i,\downarrow}^\dagger$, $c_{i\uparrow} \rightarrow c_{i\uparrow}$ inverts the sign of H_U [9]. At half-filling this allows to transform solutions of the positive- U model into those of the negative- U model. This transformation implies that the single-particle spectral function at half-filling is identical for positive and negative U . In the appendix some of the operators introduced in this work and their transformation properties under these transformations are listed.

We proceed with the calculation of the single-particle Green's function. As a first step, following Hubbard [1], we split the electron annihilation operator into the two eigenoperators of the interaction part:

$$c_{i,\sigma} = c_{i,\sigma} n_{i,\bar{\sigma}} + c_{i,\sigma} (1 - n_{i,\bar{\sigma}})$$

$$= \hat{d}_{i,\sigma} + \hat{c}_{i,\sigma}. \quad (2)$$

These obey $[\hat{d}_{i,\sigma}, H_U] = \frac{U}{2} \hat{d}_{i,\sigma}$ and $[\hat{c}_{i,\sigma}, H_U] = -\frac{U}{2} \hat{c}_{i,\sigma}$. Next, we consider the commutators of these 'effective particles' with the kinetic energy. After some algebra, thereby using the identity $n_{i,\sigma} = \frac{n_i}{2} + \sigma S_i^z$, we find:

$$[\hat{c}_{i,\uparrow}, H_t] = -t \sum_{j \in N(i)} [(1 - \frac{\langle n \rangle}{2}) c_{j,\uparrow} + (c_{j,\uparrow} S_i^z + c_{j,\downarrow} S_i^-)$$

$$- \frac{1}{2} c_{j,\uparrow} (n_i - \langle n \rangle) + c_{j,\downarrow}^\dagger c_{i,\downarrow} c_{i,\uparrow}],$$

$$[\hat{d}_{i,\uparrow}, H_t] = -t \sum_{j \in N(i)} [\frac{\langle n \rangle}{2} c_{j,\uparrow} - (c_{j,\uparrow} S_i^z + c_{j,\downarrow} S_i^-)$$

$$+ \frac{1}{2} c_{j,\uparrow} (n_i - \langle n \rangle) - c_{j,\downarrow}^\dagger c_{i,\downarrow} c_{i,\uparrow}]. \quad (3)$$

Here $N(i)$ denotes the z nearest neighbors of site i . Keeping only the first term in each of the square brackets on the r.h.s. (as we will do for the remainder of this section) reproduces the Hubbard I approximation. We specialize to half-filling ($\langle n_{i,\sigma} \rangle = 1/2$) and introduce the Green's functions

$$G_{\alpha,\beta}(\vec{k}, t) = -i \langle T \alpha_{\mathbf{k},\sigma}^\dagger(t) \beta_{\mathbf{k},\sigma} \rangle, \quad (4)$$

where $\alpha, \beta \in \{\hat{c}, \hat{d}\}$. Then, using the anticommutator relations $\{\hat{d}_{i,\sigma}^\dagger, \hat{d}_{i,\sigma}\} = n_{i\bar{\sigma}}$, $\{\hat{c}_{i,\sigma}^\dagger, \hat{c}_{i,\sigma}\} = (1 - n_{i\bar{\sigma}})$,

$\{\hat{d}_{i,\sigma}^\dagger, \hat{c}_{i,\sigma}\} = \{\hat{c}_{i,\sigma}^\dagger, \hat{d}_{i,\sigma}\} = 0$ we obtain the following equations of motion:

$$i\partial_t G_{\hat{c},\hat{c}} = \frac{1}{2} \delta(t) + \frac{\epsilon_{\mathbf{k}} - U}{2} G_{\hat{c},\hat{c}} + \frac{\epsilon_{\mathbf{k}}}{2} G_{\hat{d},\hat{c}},$$

$$i\partial_t G_{\hat{d},\hat{c}} = \frac{\epsilon_{\mathbf{k}}}{2} G_{\hat{c},\hat{c}} + \frac{\epsilon_{\mathbf{k}} + U}{2} G_{\hat{d},\hat{c}},$$

$$i\partial_t G_{\hat{c},\hat{d}} = \frac{\epsilon_{\mathbf{k}} - U}{2} G_{\hat{c},\hat{d}} + \frac{\epsilon_{\mathbf{k}}}{2} G_{\hat{d},\hat{d}},$$

$$i\partial_t G_{\hat{d},\hat{d}} = \frac{1}{2} \delta(t) + \frac{\epsilon_{\mathbf{k}}}{2} G_{\hat{c},\hat{d}} + \frac{\epsilon_{\mathbf{k}} + U}{2} G_{\hat{d},\hat{d}}. \quad (5)$$

Taking into account that the ordinary electron Green's function G and the Green's function called Γ by Hubbard [1] can be written as

$$G = G_{\hat{c},\hat{c}} + G_{\hat{c},\hat{d}} + G_{\hat{d},\hat{c}} + G_{\hat{d},\hat{d}},$$

$$\Gamma = G_{\hat{d},\hat{c}} + G_{\hat{d},\hat{d}}, \quad (6)$$

the resulting equations of motions are precisely those derived in the Hubbard-I approximation:

$$i\partial_t G = \delta(t) + (\epsilon_{\mathbf{k}} - \frac{U}{2}) G + U \Gamma,$$

$$i\partial_t \Gamma = \frac{1}{2} (\delta(t) + \epsilon_{\mathbf{k}} G + U \Gamma). \quad (7)$$

The present formulation, on the other hand, allows for an appealing physical interpretation of the Hubbard-I approximation: we introduce free Fermion operators $h_{\mathbf{k},\sigma}^\dagger$ and $d_{\mathbf{k},\sigma}^\dagger$, which correspond to 'holes' and 'double occupancies'. The Hubbard operators are identified with these as follows:

$$\hat{c}_{\mathbf{k},\sigma} \rightarrow \frac{1}{\sqrt{2}} h_{-\mathbf{k},\sigma}^\dagger$$

$$\hat{d}_{\mathbf{k},\sigma} \rightarrow \frac{1}{\sqrt{2}} d_{\mathbf{k},\sigma}. \quad (8)$$

Then, we can formally obtain the set of equations of motion (5) from the following Hamiltonian for the holes and double occupancies:

$$H_{eff} = \sum_{\mathbf{k},\sigma} (\frac{\epsilon_{\mathbf{k}} + U}{2} d_{\mathbf{k},\sigma}^\dagger d_{\mathbf{k},\sigma} - \frac{\epsilon_{\mathbf{k}} - U}{2} h_{\mathbf{k},\sigma}^\dagger h_{\mathbf{k},\sigma})$$

$$+ \sum_{\mathbf{k}} (\frac{\epsilon_{\mathbf{k}}}{2} d_{\mathbf{k},\uparrow}^\dagger h_{-\mathbf{k},\downarrow}^\dagger + H.c.). \quad (9)$$

The Hamiltonian (9) is a quadratic form and readily solved by Bogoliubov transformation:

$$\gamma_{-\mathbf{k},\sigma} = u_{\mathbf{k}} d_{\mathbf{k},\sigma} + v_{\mathbf{k}} h_{-\mathbf{k},\bar{\sigma}}^\dagger,$$

$$\gamma_{+\mathbf{k},\sigma} = -v_{\mathbf{k}} d_{\mathbf{k},\sigma} + u_{\mathbf{k}} h_{-\mathbf{k},\bar{\sigma}}^\dagger, \quad (10)$$

to yield the familiar dispersion relation

$$E_{\pm}(\mathbf{k}) = \frac{1}{2} [\epsilon_{\mathbf{k}} \pm \sqrt{\epsilon_{\mathbf{k}}^2 + U^2}]. \quad (11)$$

To compute the spectral weight of the two bands we use $c_{\mathbf{k},\sigma} = \frac{1}{\sqrt{2}}(d_{\mathbf{k},\sigma} + h_{-\mathbf{k},\bar{\sigma}}^{\dagger})$, whence

$$\begin{aligned} Z_{\pm}(\mathbf{k}) &= \frac{1}{2}(u_{\mathbf{k}} \mp v_{\mathbf{k}})^2. \\ &= \frac{1}{2} \left(1 \pm \frac{\epsilon_{\mathbf{k}}}{\sqrt{\epsilon_{\mathbf{k}}^2 + U^2}} \right). \end{aligned} \quad (12)$$

Again, this is the correct Hubbard-I result. The above discussion shows the physical content of the Hubbard-I approximation: the Hamiltonian (9) describes Fermionic particle-like and hole-like charge fluctuations, created by $d_{\mathbf{k},\sigma}^{\dagger}$ and $h_{-\mathbf{k},\bar{\sigma}}^{\dagger}$, respectively. These ‘live’ in a background of singly occupied sites. Particle-like and hole-like charge fluctuations are created in pairs on nearest neighbors, and individually can hop between nearest neighbors. The hopping integral for the hole-like particle has opposite sign as that for the electron-like fluctuation as it has to be, and the hopping integrals for both effective particles are 1/2 times that for the ordinary electrons: this reflects the fact that due to the Pauli principle (say) a spin up electron added to a ‘background’ of singly occupied sites can propagate to a neighboring site only with a probability of 1/2 (we are neglecting any spin correlations of the background of singly occupied sites). The factor of $1/\sqrt{2}$ in (8) is due to the fact that $\langle \hat{c}_{i,\sigma}^{\dagger} \hat{c}_{i,\sigma} \rangle = 1/2$. Finally, the particle which stands for the double occupancy has an energy of formation of $U/2$, the hole-like particle has an energy of $-U/2$. As already mentioned, the Hubbard I approximation therefore describes the splitting of the physical electron into two new effective particles which carry with them information on the ‘environment’ in which the electron has been created. One of them ($d_{\mathbf{k},\sigma}$) moves between sites occupied by an electron of opposite spin, the other one ($h_{-\mathbf{k},\bar{\sigma}}$) between empty sites. This is a quite appealing physical idea, but the above formulation also very clearly highlights the weak points of the Hubbard-I approximation. In addition to the mere truncation of the commutators (3), which is an uncontrolled approximation, these are the following: adopting this picture we would have to assume that the states $h_{i,\uparrow}^{\dagger} d_{j,\uparrow}^{\dagger} |0\rangle$ and $h_{i,\downarrow}^{\dagger} d_{j,\downarrow}^{\dagger} |0\rangle$ are distinguishable (and in fact orthogonal to one another). This, however, is in general not the case: both states have one double occupancy on site j and a hole on site i , and the only difference is that they have been created in different ways. In fact, using (8) we find for their overlap

$$\begin{aligned} \langle d_{j,\downarrow} h_{i,\downarrow} h_{i,\uparrow}^{\dagger} d_{j,\uparrow}^{\dagger} \rangle &= -4 \langle S_i^- S_j^+ \rangle \\ &= -\frac{8}{3} \langle \vec{S}_i \cdot \vec{S}_j \rangle, \end{aligned} \quad (13)$$

where we have assumed a rotationally invariant ground state in the second line. The Hubbard-like approximation

scheme thus should work only for a state with vanishing spin correlations - we will therefore henceforth assume the spin correlation function $\langle \vec{S}_i \cdot \vec{S}_j \rangle$ to be zero.

A second problem is, that the effective Fermions have to obey a kind of hard-core constraint - a site cannot be simultaneously occupied by a hole and a double-occupancy. This constraint is not accounted for in the derivation of the Hubbard-I approximation: the equations of motion are obtained from the Hamiltonian (9) by treating the h and d as ordinary free Fermion operators. This problem is the source of the violation of certain sum-rules when the Hubbard-I approximation is applied in the doped case, see the discussion given by Avella *et al.* [10].

One last remark is that the commutators (3) are invariant under the particle-hole transformation, i.e. they are transformed into each others Hermitian conjugate. This remains true for the truncated commutators, which give the Hubbard-I approximation, so that the spectral function obtained from this is particle-hole symmetric. This can also be verified directly using (11) and (12). Finally, the spectral function is manifestly invariant under sign change of U , as it has to be.

III. EXTENSION OF THE HUBBARD I APPROXIMATION

We now want to try and derive an improved version of the Hubbard-I approximation. Thereby we will address neither the problem of nonorthogonality of different hole/double-occupancy configurations nor the hard-core constraint - instead, in this work we will restrict ourselves entirely to an approximate way of treating the omitted terms in the commutator relations (3). We expect that the present approximation is reasonable for large U (where the density of holes/double occupancies is small whence the hard-core constraint is of little importance) and weak spin correlations (where the nonorthogonality problem is small). Throughout we stick to the case of half-filling and no spin polarization, $\langle n_{i,\sigma} \rangle = 1/2$. We return to the basic commutator relations (3) and consider the terms on the r.h.s. which are omitted in the Hubbard-I scheme. The second term in the square bracket is the Clebsch-Gordan contraction of the spin-1/2 operator $c_{j,\sigma}$ and the spin-1 operator \vec{S}_i into yet another spin-1/2 operator - it describes the coupling of the created hole/annihilated double occupancy to spin excitations. This term may be expected to be the most important one in the limit of large positive U . The third term describes in an analogous way the coupling to density fluctuations, whereas the last term describes the coupling to the so-called η -pair excitation [11]. One may expect that in the case of *negative* U the last two terms are the important ones.

In keeping with the basic idea of the Hubbard approximations, namely to treat the dominant interaction terms

exactly, we split also the composite operator into eigenoperators of the U -term and define:

$$\begin{aligned}\hat{C}_{i,j,\uparrow} &= \hat{c}_{j,\uparrow} S_i^z + \hat{c}_{j,\downarrow} S_i^- - \frac{1}{2} \tilde{n}_i \hat{c}_{j,\uparrow} + c_{i,\downarrow} c_{i,\uparrow} \hat{d}_{j,\downarrow}^\dagger, \\ \hat{D}_{i,j,\uparrow} &= \hat{d}_{j,\uparrow} S_i^z + \hat{d}_{j,\downarrow} S_i^- - \frac{1}{2} \tilde{n}_i \hat{d}_{j,\uparrow} + c_{i,\downarrow} c_{i,\uparrow} \hat{c}_{j,\downarrow}^\dagger,\end{aligned}\quad (14)$$

where $\tilde{n}_i = n_i - \langle n \rangle$. Under the positive/negative U transformation we have for example $\hat{c}_{j,\uparrow} S_i^z + \hat{c}_{j,\downarrow} S_i^- \rightarrow \frac{1}{2} \tilde{n}_i \hat{d}_{j,\uparrow} + c_{i,\downarrow} c_{i,\uparrow} \hat{c}_{j,\downarrow}^\dagger$, i.e. keeping the at first sight unimportant (for positive U) terms involving density and pairing fluctuations is crucial for maintaining the exact symmetry under sign change of U . We then have

$$\begin{aligned}[\hat{D}_{i,j,\sigma}, H_U] &= \frac{U}{2} \hat{D}_{i,j,\sigma}, \\ [\hat{C}_{i,j,\sigma}, H_U] &= -\frac{U}{2} \hat{C}_{i,j,\sigma}, \\ [\hat{c}_{i,\uparrow}, H_t] &= -t \sum_{j \in N(i)} \left[\frac{1}{2} c_{j,\uparrow} + \hat{C}_{i,j,\sigma} + \hat{D}_{i,j,\sigma} \right], \\ [\hat{d}_{i,\uparrow}, H_t] &= -t \sum_{j \in N(i)} \left[\frac{1}{2} c_{j,\uparrow} - \hat{C}_{i,j,\sigma} - \hat{D}_{i,j,\sigma} \right].\end{aligned}\quad (15)$$

The operators $\hat{C}_{i,j,\sigma}$ and $\hat{D}_{i,j,\sigma}$ may be thought of describing ‘composite objects’ consisting of a charge fluctuation and a spin-, density- or η -excitation on a nearest neighbor. Ultimately these composite operators carry the quantum numbers of a single electron, i.e. spin 1/2 and charge 1. We also note that under particle-hole transformation

$$\hat{C}_{i,j,\sigma} \rightarrow e^{i\mathbf{Q} \cdot \mathbf{R}_i} \hat{D}_{i,j,\sigma}^\dagger \quad (16)$$

i.e. the composite particles transform in the same way as the $\hat{c}_{i,\sigma}$ and $\hat{d}_{i,\sigma}$. Moreover, the commutators (15) are invariant under particle-hole transformation, i.e. this transformation transforms them into each others Hermitian conjugates.

We now enlarge the set of Green’s functions by allowing $\alpha, \beta \in \{\hat{c}, \hat{d}, \hat{C}, \hat{D}\}$ in (4); in the language of the ‘effective Fermions’ this means that we are introducing additional Fermions corresponding to the composite objects. To obtain a closed system of equations of motion for these Green’s functions, we need equations for the $G_{\hat{C}\hat{c}}$ and $G_{\hat{D}\hat{d}}$. As a first step we turn to the commutators $[\hat{C}_{i,j,\sigma}, H_t]$ and $[\hat{D}_{i,j,\sigma}, H_t]$. Here we have to distinguish three cases (see Figure 1):

- the hopping term may act along the bond (i, j) and transport the hole back from j to i .
- it may transport the hole even further away from i
- it may transport the spin- density- or η -excitation away from site i .

If we want to restrict ourselves to the 4 types of operators $\hat{C}_{i,j,\sigma}$, $\hat{D}_{i,j,\sigma}$, $\hat{c}_{i,\sigma}$ and $\hat{d}_{i,\sigma}$, we have to neglect the contributions from the processes b and c. These processes would produce ‘strings’ of excitations along a path

of length 2 lattice spacings, and we would have to introduce even more complicated operator products to describe these. Restricting ourselves to processes of the type a, i.e. replacing $H_t \rightarrow -t \sum_{\sigma} (c_{i,\sigma}^\dagger c_{j,\sigma} + H.c.)$, straightforward computation [12] gives the surprisingly simple result

$$\begin{aligned}[\hat{C}_{i,j,\uparrow}, H_t] &= \frac{3t}{2} \hat{D}_{j,i,\uparrow} + \frac{t}{2} \hat{C}_{j,i,\uparrow} - \frac{3t}{4} (\hat{c}_{i,\uparrow} - \hat{d}_{i,\uparrow}), \\ [\hat{D}_{i,j,\uparrow}, H_t] &= \frac{3t}{2} \hat{C}_{j,i,\uparrow} + \frac{t}{2} \hat{D}_{j,i,\uparrow} - \frac{3t}{4} (\hat{c}_{i,\uparrow} - \hat{d}_{i,\uparrow}).\end{aligned}\quad (17)$$

Again, these relations are particle-hole invariant, i.e. they are turned into each others Hermitian conjugates by particle-hole transformation. In passing we note that had we reduced the operators $\hat{C}_{i,j,\uparrow}$ and $\hat{D}_{i,j,\uparrow}$ to comprise only the terms involving spin excitations (as might seem appropriate in the case of large positive U), the commutators would have been much more complicated and in fact the ‘Hamilton matrix’ H_k to be defined below would have been non-Hermitian.

Next, we need the anticommutators

$$\begin{aligned}\{\hat{C}_{i,j,\uparrow}, \hat{c}_{l,\uparrow}^\dagger\} &= \delta_{j,l} [S_i^z S_j^z + S_i^- S_j^+ + \frac{\tilde{n}_i \tilde{n}_j}{4} \\ &\quad + c_{j,\uparrow}^\dagger c_{j,\downarrow}^\dagger c_{i,\uparrow} c_{i,\downarrow}] \\ &\quad + \delta_{j,l} \left[\frac{1}{2} S_i^z - \frac{1}{4} \tilde{n}_i - \frac{1}{2} (\tilde{n}_i S_j^z + \tilde{n}_j S_i^z) \right] \\ &\quad + \delta_{i,l} [\hat{c}_{j,\downarrow} \hat{c}_{i,\downarrow}^\dagger - \hat{d}_{i,\downarrow} \hat{d}_{j,\downarrow}^\dagger] \\ \{\hat{D}_{i,j,\uparrow}, \hat{c}_{l,\uparrow}^\dagger\} &= \delta_{i,l} [\hat{c}_{j,\downarrow} \hat{d}_{i,\downarrow}^\dagger + \hat{d}_{j,\downarrow}^\dagger \hat{c}_{i,\downarrow}]\end{aligned}\quad (18)$$

Taking the expectation value in the ground state most of the terms vanish on the basis of symmetries: $\hat{c}_{j,\downarrow} \hat{d}_{i,\downarrow}^\dagger + \hat{d}_{j,\downarrow}^\dagger \hat{c}_{i,\downarrow}$ vanishes due to inversion symmetry of the ground state, $\hat{c}_{j,\downarrow} \hat{c}_{i,\downarrow}^\dagger - \hat{d}_{i,\downarrow} \hat{d}_{j,\downarrow}^\dagger$ and \tilde{n}_i vanish due to particle-hole symmetry at half-filling. All terms containing unpaired spin operators vanish if we assume that the ground state is invariant under spin rotations (which excludes ferro- or antiferromagnetic solutions). Finally we obtain:

$$\begin{aligned}\langle \{\hat{C}_{i,j,\uparrow}, \hat{c}_{l,\uparrow}^\dagger\} \rangle &= \delta_{j,l} (\vec{S}_i \cdot \vec{S}_j + \frac{\tilde{n}_i \tilde{n}_j}{4} + c_{i,\uparrow}^\dagger c_{i,\downarrow}^\dagger c_{j,\uparrow} c_{j,\downarrow}), \\ \langle \{\hat{D}_{i,j,\uparrow}, \hat{c}_{l,\uparrow}^\dagger\} \rangle &= 0.\end{aligned}\quad (19)$$

It is easy to see that the expressions whose expectation values are taken are invariant under particle-hole transformation, and under the positive/negative U transformation we have:

$$\begin{aligned}\frac{\tilde{n}_i \tilde{n}_j}{4} &\leftrightarrow S_i^z S_j^z, \\ c_{i,\uparrow}^\dagger c_{i,\downarrow}^\dagger c_{j,\uparrow} c_{j,\downarrow} &\leftrightarrow S_i^+ S_j^-.\end{aligned}\quad (20)$$

The expectation value of the anticommutator would be invariant under this positive/negative- U symmetry.

For large positive U the terms $\frac{\tilde{n}_i \tilde{n}_j}{4}$ and $\dagger_{i,\uparrow} c_{i,\downarrow}^\dagger c_{j,\uparrow} c_{j,\downarrow}$ have a negligible expectation value and the only important term comes from the spin correlation. In keeping with our above remarks concerning the role of spin correlations in the Hubbard I approximation we will henceforth take the r.h.s. of (19) to be zero. As was discussed above, the Hubbard-I approximation implicitly assumes $\langle \tilde{S}_i \cdot \tilde{S}_j \rangle = 0$, and we will therefore keep this value also in (19). We will discuss the consequences of not making this approximation later on.

Using the above commutators and (expectation values of) anticommutators we are now in a position to set up a closed system of equations of motion. In the following we give explicit formulas only for a 1D chain with nearest-neighbor hopping, but the generalization to higher di-

mensions and/or longer range hopping integrals will be self-evident. We introduce the Fourier transforms

$$\hat{C}_{\pm,\sigma}(\mathbf{k}) = \sqrt{\frac{4}{3N}} \sum_j e^{i\mathbf{k} \cdot \tilde{\mathbf{R}}_j} \hat{C}_{j,j\pm 1,\sigma},$$

(and analogously for the \hat{D} 's) and define the vector $\vec{G}_c = (G_{\hat{c}\hat{c}}, G_{\hat{d}\hat{c}}, G_{\hat{c}+, \hat{c}}, G_{\hat{c}-, \hat{c}}, G_{\hat{D}+, \hat{c}}, G_{\hat{D}-, \hat{c}})$. Here \hat{C}_{\pm} is shorthand for $\hat{C}_{\pm,\sigma}(\mathbf{k})$. Combining (3), (14) and (17), and performing a spatial Fourier transformation the equations of motion are readily found to be

$$(i\partial_t - H_k) \vec{G}_c = \delta(t) B_c \quad (21)$$

where the Hermitian matrix H_k is given by

$$H_k = \begin{pmatrix} \frac{\epsilon_{\mathbf{k}} - U}{2} & , & \frac{\epsilon_{\mathbf{k}}}{2} & , & -\tilde{t}e^{-ik_x/2} & , & -\tilde{t}e^{ik_x/2} & , & -\tilde{t}e^{-ik_x/2} & , & -\tilde{t}e^{ik_x/2} \\ \frac{\epsilon_{\mathbf{k}}}{2} & , & \frac{\epsilon_{\mathbf{k}+U}}{2} & , & \tilde{t}e^{-ik_x/2} & , & \tilde{t}e^{ik_x/2} & , & \tilde{t}e^{-ik_x/2} & , & \tilde{t}e^{ik_x/2} \\ -\tilde{t}e^{ik_x/2} & , & \tilde{t}e^{ik_x/2} & , & -\frac{U}{2} & , & \frac{t}{2} & , & 0 & , & \frac{3t}{2} \\ -\tilde{t}e^{-ik_x/2} & , & \tilde{t}e^{-ik_x/2} & , & \frac{t}{2} & , & -\frac{U}{2} & , & \frac{3t}{2} & , & 0 \\ -\tilde{t}e^{ik_x/2} & , & \tilde{t}e^{ik_x/2} & , & 0 & , & \frac{3t}{2} & , & \frac{U}{2} & , & \frac{t}{2} \\ -\tilde{t}e^{-ik_x/2} & , & \tilde{t}e^{-ik_x/2} & , & \frac{3t}{2} & , & 0 & , & \frac{t}{2} & , & -\frac{U}{2} \end{pmatrix}$$

and $B_c = (\frac{1}{2}, 0, 0, 0, 0, 0)$. The equation system (21) can be solved for each momentum and frequency by using the spectral resolution of the Hamilton matrix H_k . This yields the Green's functions $G_{\hat{c}\hat{c}}$ and $G_{\hat{d}\hat{c}}$ for each momentum and frequency. In an analogous way we can also derive an equation system for $G_{\hat{c}\hat{d}}$ and $G_{\hat{d}\hat{d}}$. Thereby the matrix H_k stays unchanged, whereas the r.h.s. is changed into $B_d = (0, 1/2, 0, 0, 0, 0)$. Finally, the full electron Green's function is obtained by adding up the four Green's functions according to (6). Upon forming the Laplace transform $G(\mathbf{k}, z)$ we finally obtain the spectral density

$$A(\mathbf{k}, \omega) = -\lim_{\eta \rightarrow 0} \frac{1}{\pi} \Im G(\mathbf{k}, \omega + i\eta). \quad (22)$$

In passing we note that this way of computing $A(\mathbf{k}, \omega)$ guarantees the validity of the sum rule

$$\int_{-\infty}^{\infty} A(\mathbf{k}, \omega) d\omega = 1. \quad (23)$$

Since the particle-hole symmetry of the relations (15), (17) and (19) in turn guarantees particle-hole symmetry of the entire spectral function, we find that the sum-rule for the particle number is fulfilled automatically:

$$\sum_{\mathbf{k}} \int_{-\infty}^0 A(\mathbf{k}, \omega) d\omega = \frac{N}{2}. \quad (24)$$

As a last remark we note that going over to higher dimensions or adding longer ranged hopping integrals poses no problem whatsoever - for each spatial dimension α we

have to add four additional rows and columns containing the $\hat{C}_{i,j}$ and $\hat{D}_{i,j}$ where i and j are nearest neighbors in $\pm\alpha$ -direction. Similarly, if we add an additional hopping integral t' between 2^{nd} or 3^{rd} nearest neighbors (the number of whom we denote by z') to the Hamiltonian, we have to add $2z'$ rows and columns, containing the $\hat{C}_{i,j}$ and $\hat{D}_{i,j}$ with 2^{nd} or 3^{rd} nearest neighbors i and j . In each case these additional rows and columns contain only mixing terms amongst themselves or with $G_{\hat{c}, \hat{c}}$ and $G_{\hat{d}, \hat{c}}$, so that the extension is completely trivial.

IV. COMPARISON WITH NUMERICS

Following the discussion in the preceding section we can calculate the full electron Green's function, including the (presumably) most important corrections over the Hubbard I approximation in the limit of weak spin correlations and large U . We now proceed to a comparison of the obtained results results for the spectral density $A(\mathbf{k}, \omega)$, with the spectral density obtained from Quantum Monte-Carlo (QMC) simulations. Thereby the temperature for the QMC simulation, $T = 0.33t$, was chosen such that the spin correlation length is only approximately 1.5 lattice spacings - the results thus are probably quite representative for the paramagnetic regime which our approximation aims to describe. Moreover, the value of $U/t = 8$ is already rather large, so that we may also hope to have a small density of holes/double occupancies and the neglect of the hard-core constraint be justified. As a general remark concerning the QMC spectra we note

that the MaxEnt procedure used for the analytic continuation to the real axis is most reliable for ‘features’ with large weight - this means that the position of tiny peaks is less accurate than that of large ones.

Figure 2 then compares the spectral density obtained from the Hubbard I approximation, our extended Hubbard approximation (EHA) and QMC simulation. The Hubbard I approximation gives only a relatively crude fit to the actual spectral density obtained by QMC. The extended Hubbard approximation, on the other hand, gives an all in all quite correct description of the spectral density. Out of the $10 = 2 + 4 + 4$ bands produced by diagonalizing H_k , only four bands do have an appreciable spectral weight. These four intense bands correspond rather well to 4 broad ‘bands’ of intense spectral weight which can be roughly identified in the QMC result. It is interesting to note that a recent strong-coupling expansion for the Hubbard model by Pairault *et al.* [13] also produced a 4-band structure, although only for the 1D model. The dispersion of the spectral weight along the bands is also reproduced quite satisfactorily by the extended Hubbard approximation. The main difference is the apparently strongly \mathbf{k} -dependent width of the spectra produced by QMC, which however is outside the scope of the present approximation, which (in the limit $\eta \rightarrow 0$) produces sharp δ -peaks without any broadening. A more severe deficiency of the EHA is, that it tends to predict too high excitation energies, resulting in a somewhat too large value of the Hubbard gap. In any way, however, the magnitude of the Hubbard gap comes out better than in the Hubbard-I approximation.

We proceed to the Hubbard model with an additional hopping integral t' between 2^{nd} nearest (i.e. (1,1)-like) neighbors. Figure 3 again compares the Hubbard I approximation, the EHA, and the results of a QMC simulation on an 8×8 lattice. The agreement between EHA and the QMC result is again quite good, the main discrepancy being again an overall overestimation of the binding energies. On the other hand, the apparent 4-band structure, the dispersion of the peak energies and the spectral weight agrees well with the numerical result. In particular, the 2 bands in inverse photoemission (i.e. $\omega > 0$) predicted by the EHA can be seen very clearly in the QMC spectra). All in all the agreement is even better than for the case $t' = 0$, which most probably is due to the fact that the spin correlations are weaker with t' , so that the assumption of an uncorrelated spin state is better justified in this case.

We proceed to the case of a hopping integral t'' between 3^{rd} nearest (i.e. (2,0)-like) neighbors. Here we have chosen $t''/t = 0.25$, because for the larger value $t''/t = 0.5$ the QMC simulation still predicted a metallic state at $U/t = 8$. Figure 4 shows the spectral functions for $t''/t = 0.25$. Again, we can roughly identify 4 bands and there is reasonable agreement for the dispersion. The weight of the quasiparticle band in photoemission near

(π, π) (at $\omega \approx -2$) is not reproduced very well by the EHA, but again the ubiquitous 4-band structure is rather clearly visible.

Next, we turn to a somewhat indirect check of the approximation. The ordinary electron creation operator is the symmetric combination of the Hubbard operators. However, we might also define the antisymmetric combination

$$\tilde{c}_{i,\sigma} = c_{i,\sigma} n_{i,\bar{\sigma}} - c_{i,\sigma}(1 - n_{i,\bar{\sigma}}). \quad (25)$$

This operator has the same quantum numbers as the original electron operator, and therefore obeys the same selection rules. It follows that when acting on the ground state, this operator probes the same final states as the electron operator, the only difference being the matrix element viz. the spectral weight of the respective peak in the spectral density. In fact the Green’s function

$$\tilde{G}(\mathbf{k}, t) = -i \langle T \tilde{c}_{\mathbf{k},\sigma}^\dagger(t) \tilde{c}_{\mathbf{k},\sigma} \rangle \quad (26)$$

can be expressed as

$$\tilde{G} = G_{cc} - G_{dc} - G_{cd} + G_{dd}. \quad (27)$$

It therefore is easy to calculate within our approximation, and comparison with the QMC result provides an additional check for our description of the electronic structure. Note that the operator $\tilde{c}_{\mathbf{k},\sigma}$ enhances the practically dispersionless bands at $\omega = \pm 6$ - since these bands now have a larger weight, their position and dispersion are more reliable than in the ‘ordinary’ photoemission spectrum. This is shown in Figure 5, where indeed quite good agreement is found between the EHA and the numerical result.

Finally, we turn to the discussion of choosing a nonvanishing expectation value of the anticommutator in (19), i.e. we assume that $\langle \{\hat{C}_{i,j,\sigma}, \hat{c}_l^\dagger\} \rangle = \delta_{j,l} x \neq 0$. This changes the rhs of the equation system (21) to $B_c = (1/2, 0, \sqrt{\frac{4}{3}}x, \dots)$ but leaves the matrix H_k unchanged. In other words, the *dispersion* of the bands, which is determined by the eigenvalues of H_k stays unchanged and only the spectral weight of the peaks changes. Moreover the sum rules (23) and (24) retain their validity also in this case. For large positive U and $n = 1$ charge fluctuations will be strongly suppressed and double occupancies will have a small probability, so that the dominant contribution to x comes from the spin correlation function $\langle \vec{S}_i \cdot \vec{S}_j \rangle$, whence we should choose $x < 0$. Assuming for example a negative x of moderate value, $x = -0.2$, then leads to little change in the calculated spectral density (see Figure 6): the same two bands which had a large spectral weight for $x = 0$ retain a large spectral weight also in this case. There is, however, a rather undesirable feature associated with the bands with small spectral weight: numerical evaluation shows, that for some

regions of \mathbf{k} -space these bands acquire a small but *negative* weight.

The physical origin of this problem is probably related to nonorthogonalities of basis states: in principle we could interpret the matrix $H_{\mathbf{k}}$ as a Hamiltonian describing (in 2D with only nearest neighbor hopping) 6 types of Fermionic ‘effective particles’. Quite generally, the anticommutator-relation $\{a, b^\dagger\} = x \neq 0$ implies that the wave functions corresponding to the Fermi operators a^\dagger and b^\dagger are non-orthogonal. While an exact overlap matrix can never have negative eigenvalues but at most develop zero eigenvalues (indicating that the set of basis states is overcomplete), any approximation to the matrix elements may lead, as an artefact of the approximation, to negative eigenvalues. Since we are using only approximate values for the overlaps, it may happen that we obtain states with a nominally negative norm, whence we can get poles of negative weight. Setting $x = 0$ throughout amounts to assuming that all our effective particles are orthogonal to one another and obviously removes the problem with nonorthogonalities. This seems reasonable, because we are neglecting overlap terms proportional to the spin correlation function already in the Hubbard-I approximation. The lesson then is basically the same as discussed already before: the Hubbard-I approximation is well defined only when applied to an ‘ideally paramagnetic’ state with no correlations of finite range, and applying it to a state with finite spin correlations represents an approximation.

V. CONCLUSION

In summary, we have investigated the most important corrections over the Hubbard-I approximation in the limit $U/t \rightarrow \infty$ and electron density $n = 1$. We have seen that the Hubbard-I approximation describes charge fluctuations on a ‘background’ of singly occupied sites, which is moreover assumed to have zero spin correlations. The charge fluctuations are point-like, and correspond to an electron moving between empty sites and an electron moving between singly occupied sites. We note that a very similar construction can also be applied to the Kondo lattice [14] and in fact reproduces the single particle spectra very well. This is probably due to the fact that the Kondo lattice has a unique ground state in the limit of zero kinetic energy, whereas the ground state of the Hubbard model is highly degenerate in the case $t = 0$.

In our extended scheme for the Hubbard model we have augmented these point-like charge fluctuations by additional ‘particles’ which are composite in character and consist of a point-like charge fluctuation together with a spin-, density-, or η -excitation. Comparison of the obtained single-particle spectral density with QMC results for a variety of systems showed a quite reasonable agree-

ment. In particular the apparent 4-band structure seen in the numerical spectra finds its natural explanation in the extended Hubbard approximation. We also note that QMC simulations where the spectra of the composite excitations have actually been computed [15], further support the present interpretation. We thus have a quite successful method of computing the full quasiparticle band structure of the Hubbard model, at least in the paramagnetic case and at half-filling.

The present scenario for the nature of the composite excitations also allows to make a connection with various theories for the hole motion in an antiferromagnet [16–21]. There, one is describing holes dressed by antiferromagnetic spin fluctuations. When acting on the Néel state the operators $\hat{C}_{i,j,\sigma}$ obviously describe precisely a hole together with a ‘spin wave’ on a nearest neighbor or, put another way, a ‘string’ of length one. The terms which were omitted from the equation of motion for the $\hat{C}_{i,j,\sigma}$ then would correspond to strings of length two and so on. While such longer-ranged strings are apparently of minor importance in the paramagnetic phase, one may expect that they become more and more important for the description of the dispersion the stronger the antiferromagnetic correlations. The relative importance of such longer ranged strings therefore may be the mechanism for the crossover from the Hubbard-I like dispersion in the paramagnetic phase to the spin-density-wave like dispersion in the antiferromagnetic phase. Similarly, one might think of formulating the entire Hubbard-I approximation also in the antiferromagnetic phase, by constructing the Hamiltonian for charge fluctuations explicitly for a Néel ordered spin background.

We thank H.-G. Evertz and W. Hanke for discussions. This work was supported by BMBF (05SB8WWA1), computations were performed at HLRS Stuttgart, LRZ München and HLRZ Jülich.

VI. APPENDIX

Transformation properties of various operators under particle-hole and positive/negative U transformation.

Operator	particle-hole	positive/negative U
$\hat{c}_{i,\uparrow}$	$e^{i\mathbf{Q}\cdot\mathbf{R}_i} \hat{d}_{i,\uparrow}^\dagger$	$\hat{d}_{i,\uparrow}$
$\hat{c}_{i,\downarrow}$	$e^{i\mathbf{Q}\cdot\mathbf{R}_i} \hat{d}_{i,\downarrow}^\dagger$	$e^{i\mathbf{Q}\cdot\mathbf{R}_i} \hat{c}_{i,\downarrow}^\dagger$
$\hat{d}_{i,\uparrow}$	$e^{i\mathbf{Q}\cdot\mathbf{R}_i} \hat{c}_{i,\uparrow}^\dagger$	$\hat{c}_{i,\uparrow}$
$\hat{d}_{i,\downarrow}$	$e^{i\mathbf{Q}\cdot\mathbf{R}_i} \hat{c}_{i,\downarrow}^\dagger$	$e^{i\mathbf{Q}\cdot\mathbf{R}_i} \hat{d}_{i,\downarrow}^\dagger$
S_i^+	$-S_i^-$	$e^{i\mathbf{Q}\cdot\mathbf{R}_i} c_{i,\uparrow}^\dagger c_{i,\downarrow}^\dagger$
S_i^-	$-S_i^+$	$e^{i\mathbf{Q}\cdot\mathbf{R}_i} c_{i,\downarrow} c_{i,\uparrow}$
S_i^z	$-S_i^z$	$\frac{1}{2}(n_i - 1)$
$n_i - 1$	$1 - n_i$	$2S_i^z$
$\hat{C}_{i,j,\uparrow}$	$e^{i\mathbf{Q}\cdot\mathbf{R}_i} \hat{C}_{i,j,\uparrow}^\dagger$	$-\hat{D}_{i,j,\uparrow}$
$\hat{C}_{i,j,\downarrow}$	$e^{i\mathbf{Q}\cdot\mathbf{R}_i} \hat{C}_{i,j,\downarrow}^\dagger$	$-e^{i\mathbf{Q}\cdot\mathbf{R}_i} \hat{D}_{i,j,\uparrow}^\dagger$

-
- [1] J. Hubbard, Proc. Roy. Soc. A **276**, 238 (1963).
 - [2] J. Hubbard, Proc. Roy. Soc. A **277**, 237 (1964); J. Hubbard, Proc. Roy. Soc. A **281**, 401 (1964).
 - [3] L. M. Roth, Phys. Rev. **184**, 451 (1969).
 - [4] G. Geipel and W. Nolting, Phys. Rev. B **38**, 2608 (1988); W. Nolting and W. Borgiel, Phys. Rev. B **39**, 6962 (1989).
 - [5] B. Mehlig, H. Eskes, R. Hayn, and M. B. J. Meinders, Phys. Rev. B **52**, 2463 (1995).
 - [6] J. Beenen and D. M. Edwards, Phys. Rev. B **52**, 13636 (1995).
 - [7] C. Gröber, M. G. Zacher, and R. Eder, condmat/9902015.
 - [8] E. Dagotto, Rev. Mod. Phys. **67**, 63 (1994).
 - [9] R. Micnas, J. Ranninger, and S. Robaszkiewicz, Rev. Mod. Phys. **62**, 113 (1990).
 - [10] A. Avella, F. Mancini, D. Villani, L. Siurakshina, V. Yu. Yushankhai, Int. Journ. Mod. Phys. B **12**, 81 (1998); see also F. Mancini, Phys. Lett. A **249**, 231 (1998).
 - [11] C. N. Yang, Phys. Rev. Lett. **63**, 2144 (1989); S. C. Zhang, Phys. Rev. Lett. **65**, 120 (1990).
 - [12] The more complicated (anti)commutators in this work were obtained by a Mathematica implementation of the Fermion algebra.
 - [13] S. Pairault, D. Senechal, and A.-M. S. Tremblay, Phys. Rev. Lett. **80**, 5389 (1998).
 - [14] R. Eder, O. Rogojanu, and G. A. Sawatzky, Phys. Rev. B **58**, 7599 (1998).
 - [15] C. Gröber, R. Eder, W. Hanke (in preparation).
 - [16] L. N. Bulaevskii, E. L. Nagaev, and D. I. Khomskii, Sov. Phys. JETP **27**, 638 (1967).
 - [17] S. A. Trugman, Phys. Rev. B **37**, 1597 (1988); *ibid.* **41**, 892 (1990).
 - [18] R. Eder and K. W. Becker, Z. Phys. B **78**, 219 (1990).
 - [19] O. P. Sushkov, Solid State Commun. **83**, 303 (1992).
 - [20] G. Reiter, Phys. Rev. B **49**, 1536 (1994).
 - [21] R. Hayn, A. F. Barabanov, J. Schulenburg, and J. Richter, Phys. Rev. B **53**, 11714 (1996).

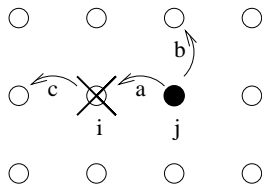


FIG. 1. Possible hopping processes which couple to $\hat{C}_{i,j,\sigma}$. The cross denotes the spin-, density- or η -excitation, the black dot the hole.

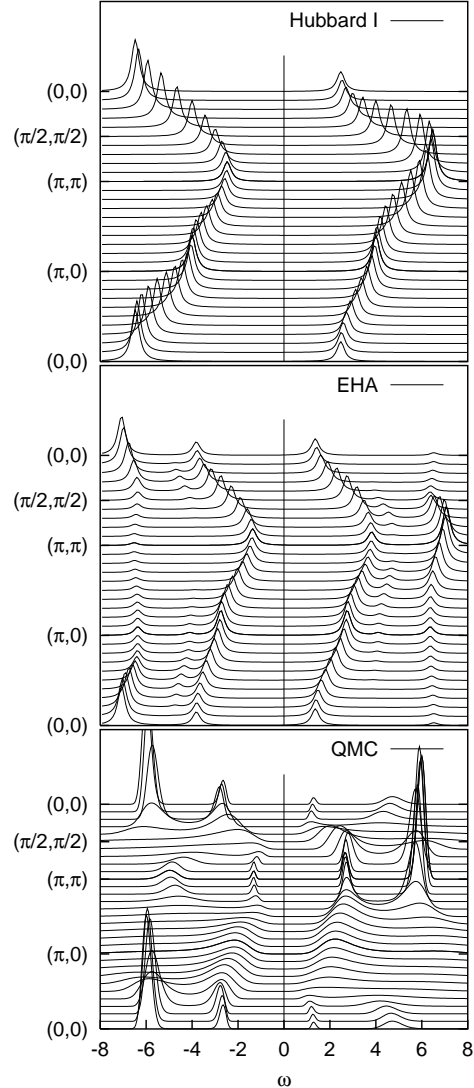


FIG. 2. Single particle spectral function for the Hubbard Model with $U/t = 8$ from the Hubbard I approximation, the extended Hubbard approximation, and QMC simulations on a 20×20 lattice at temperature $T = t/3$. In this as well as in all following figure, the approximate spectra have been given an artificial Lorentzian broadening $\eta = 0.20t$. To compensate for the stronger broadening the QMC spectra have been multiplied by an additional factor of 2.

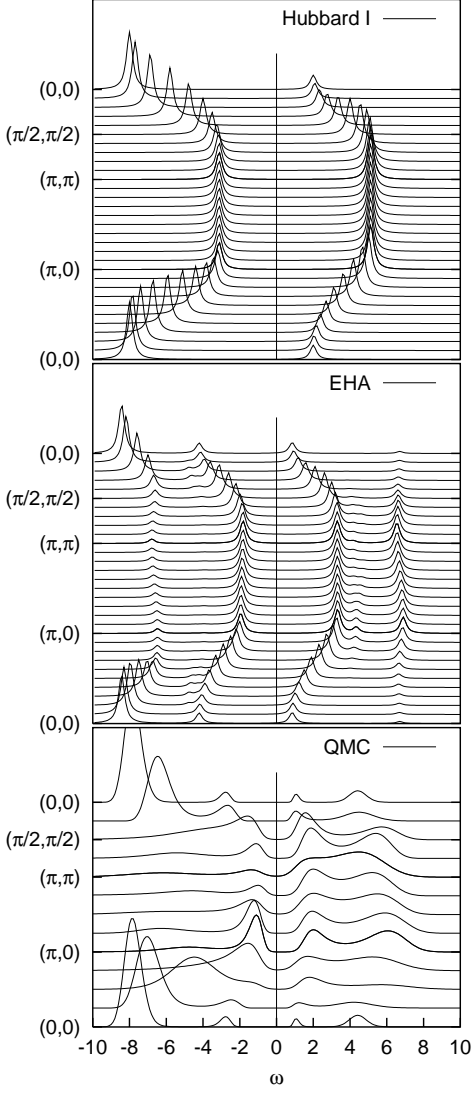


FIG. 3. Single particle spectral function for the Hubbard Model with $U/t = 8$, $t' = t/2$ from the Hubbard I approximation, the extended Hubbard approximation, and QMC simulations on an 8×8 lattice at temperature $T = t/3$. To compensate for the stronger broadening the QMC spectra have been multiplied by an additional factor of 4.

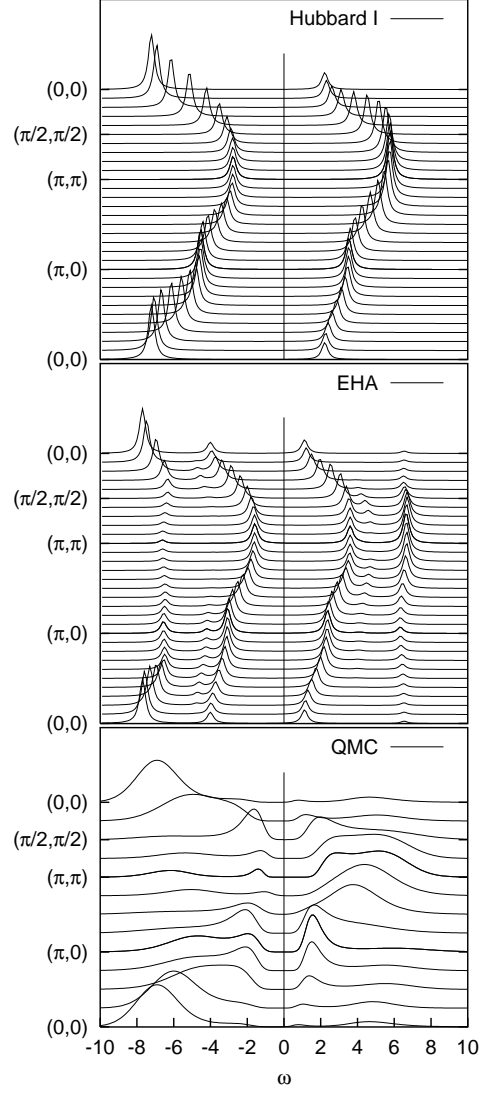


FIG. 4. Single particle spectral function for the Hubbard Model with $U/t = 8$, $t'' = t/4$ from the Hubbard I approximation, the extended Hubbard approximation, and QMC simulations on an 8×8 lattice at temperature $T = t/3$. To compensate for the stronger broadening the QMC spectra have been multiplied by an additional factor of 4.

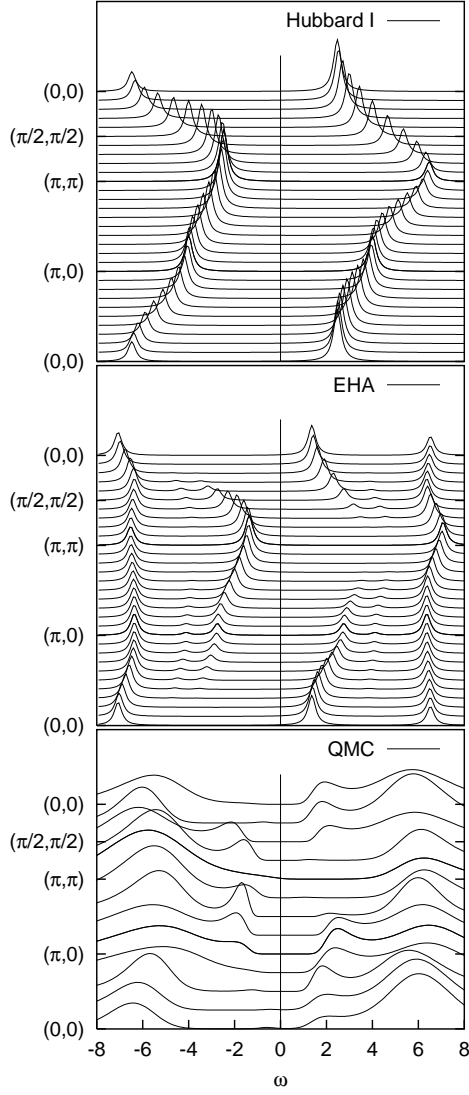


FIG. 5. Spectral function of the \tilde{c} -operator for the Hubbard Model with $U/t = 8$ from the Hubbard I approximation, the extended Hubbard approximation, and QMC simulations on an 8×8 lattice at temperature $T = t/3$. To compensate for the stronger broadening the QMC spectra have been multiplied by an additional factor of 4.

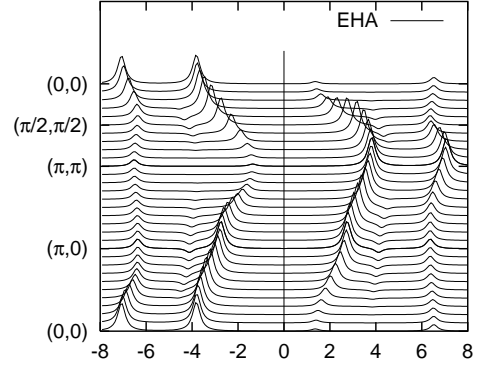


FIG. 6. Spectral function calculated with the extended Hubbard approximation for $x = -0.2$.